

A REAPPRAISAL OF CONTAINMENT SAFETY UNDER HYDROGEN DETONATION

Delichatsios¹, M.A., Fardis, M.N.²

¹FireSERT, University of Ulster at Jordanstown, Newtownabbey, BT37OQB

²Dept of Civil Engineering, University of Patras, Greece

ABSTRACT

The response of a typical steel-lined reinforced concrete nuclear reactor containment to postulated internal hydrogen detonations is investigated by detailed axisymmetric non-linear dynamic finite element analysis. The wall pressure histories are calculated for hydrogen detonations using a technique that reproduces the sharp discontinuity at the shock front. The pressure results can be applied to geometrically similar vessels. The analysis indicates that the response is more sensitive to the point of initiation than to the strength of the detonation. Approximate solutions based on a pure impulse assumption where the containment is modelled as a single-degree-of freedom (SDOF) system may be seriously unconservative. This work becomes relevant because new nuclear reactors are foreseen as a primary source of hydrogen supply.

INTRODUCTION

Hydrogen release after an accident in a nuclear reactor can lead to severe damages of fire containment. Although there is large uncertainty regarding the amount of hydrogen that can be produced inside the containment, a combination of different sources seems capable of generating within a period of several hours to a few days enough hydrogen to make the containment atmosphere flammable or even detonable[1]. It is important to emphasize that this work becomes relevant as new nuclear reactors are proposed to be primary source of hydrogen supply [15].

The dispersion and diffusion of hydrogen, the presence of ignition success and the overall hydrogen concentration in the containment will determine the burning behaviour of hydrogen. If ignition occurs prior to mixing with the containment atmosphere, the hydrogen burns as a diffusion flame (non-premixed combustion). For complete dispersion and mixing of hydrogen, ignition will lead to a deflagration if the uniform concentration of hydrogen exceeds the lower limit of flammability. Within the range of typical post-accident conditions the lower flammability limit is nearly independent of the amount of steam and of the containment pressure and temperature, and varies from 4 to 9% hydrogen volume, depending on the direction of flame propagation[12]. Due to the large number of possible ignition sources in the containment volume, hydrogen will most likely burn gradually, as it accumulates beyond the flammability limit. In the very unlikely event that hydrogen will accumulate without ignition to levels beyond the "lower detonation limit", which is 18.2% for hydrogen-air mixtures, then the final hydrogen combustion may accelerate into a detonation[12].

Deflagrations are characterized by slow subsonic propagation of a flame front, heating of the unburned gas to auto-ignition by thermal diffusion from the burned gas, and a slow but uniform rise in the pressure and temperature of the gas by the heat released from the combustion. The resulting loading on the containment is quasistatic. On the other hand, a detonation produces a shock wave driven and sustained by the chemical energy released from the chemical reaction. The shock wave and the reaction propagate together in the unburned gas, at a speed which exceeds that of sound in the burned medium, ie, of the order of 1500-2000 m/sec. The shock front is characterized by an abrupt increase in pressure, temperature and density of the gas and by a net forward movement of the gas particles. The pressure is maximum at the shock front and decays fast behind it. Shock reflection produces a large pressure on the wall (eg, 2 or 3 times the incident pressure for normal incidence), and generates a purely mechanical wave which propagates inwards in the already burnt gas until it interacts with another wave produced by reflection elsewhere. The result is a complex pattern of waves propagating within the containment volume and colliding with each other, with the walls and with internal obstacles. The associated dynamic pressures can be so large that failure of several

engineered safety systems and even core dispersal within the containment are possible. If such a catastrophic sequence of events does occur, the containment structures will be the last line of defence against early release of radioactive fission products to the atmosphere.

Accumulation of hydrogen without ignition to a detonable concentration is very unlikely. In this paper, however, we hypothesize a detonation of a uniform detonable mixture filling the volume of a large dry containment typical of pressurized water reactors, and we investigate the effects of the detonation on the containment structure. First, a numerical model for the axisymmetric hydrogen detonation problem is described and used to predict containment wall pressure histories in terms of characteristic detonation parameters and containment initial conditions. These pressure histories are then used as input to axisymmetric non-linear dynamic Finite Element analysis of the containment response.

The containment studied here is an actual steel-lined reinforced concrete structure, consisting of a cylinder with an internal radius of 67.5ft (20.57m) and 148ft (45.11m) height, capped by a hemispherical dome[6].

DYNAMIC WALL PRESSURES RESULTING FROM HYDROGEN DETONATION

Prediction of the wall pressure histories produced by the postulated hydrogen detonation requires solution of unsteady non-linear gas-dynamics equations, including combustion, in order to determine the time-histories of flow quantities (pressure, temperature, density and particle velocity) throughout the containment volume. Ref [4] presents in detail the application of the random-choice technique (originally developed in Refs [2] and [8] for purely mechanical shocks and modified in Ref. [4] to incorporate the chemical reactions) to numerically solve this problem. Unlike Finite Difference techniques, which suffer from artificial damping, the random choice method can reproduce exactly sharp discontinuities of the flow, such as shock fronts.

The principle of the random-choice technique can be illustrated in the simplest one-dimensional geometry: both space and time are discretized, and the field variables at time t are propagated to $t+\Delta t$ and the sequence of solutions to the individual Riemann problems can be considered as a continuous in space exact solution. To find the values of the field variables at the discrete grid points, the "exact" solution in each interval at $t+\Delta t$ is sampled pseudorandomly according to Ref. [2], the sample values being assigned to the midpoint of the interval, and the solution being approximated by a piecewise constant. The procedure is repeated in the next time step using space intervals defined by the midpoints. Because the chemical reaction rates are large, it is assumed that the reaction zone has zero thickness and the detonation is modelled as a sharp discontinuity which travels relative to the burnt medium with a speed equal to that of sound in the latter, changing the un-burnt gas into a completely burnt one. In the numerical calculation the detonation front is propagated from one point to the next, again by pseudorandom sampling of a point within the associated space interval [4].

One dimensional versions (i.e. planar and spherical) of the computational procedure were implemented and verified against exact analytical solutions [4]. The axisymmetric version was verified by comparing its results for a spherical geometry and initiation at the centre to those of the one-dimensional spherical version. Elastically deforming walls were introduced in the one-dimensional programme and the effects of wall deformability were studied by solving the coupled equations of the gas dynamics and wall motion. Parametric studies were performed in which the wall stiffness was increased or decreased by two orders of magnitude with respect to its reference value. It was found that the effect of wall deformability on wall pressure was less than 1%. This small effect can be explained by the very large difference between the velocity of the vibrating wall and that of the incident wave.

For the numerical determination of the detonation wall pressure histories in the containment under study, it is assumed that:

1. the hydrogen concentration is constant throughout the containment volume. This assumption is justified by the lack of containment compartmentalization and by the operation of fans and sprays during an accident. It may take a considerable time period to reach uniform concentrations [16].
2. there are no obstacles inside the containment,
3. combustion starts as a detonation at a point on the containment axis and propagates in an axisymmetric manner,
4. no energy exchange with the walls takes place in the short duration of the phenomenon,
5. the mixture of gases inside the containment behaves as an ideal gas with gas constant γ (ratio of specific heats) equal to 1.4, and
6. the containment walls are rigid.

Due to the previous simplifications (items 4 and 5, in particular), computed wall pressures, P , at a given point in space and time are proportional to the initial containment pressure, P_o , and depend only on the point of detonation initiation and on the dimensionless heat release rate, q/RT_o , where q = energy released per unit volume by the hydrogen-oxygen reaction, R = universal gas constant, equal to 8.31 kJ/Kg.mole^oK, and T_o = initial absolute temperature. If the hydrogen volumetric percentage, C_{H_2} is less than stoichiometric and T_o is ^oK, the dimensionless heat release rate equals $290 C_{H_2}/T_o$. In the calculations, two values of the dimensionless heat release rate are considered. One at the floor centre and the second at approximately the containment mid-height. Since the bottom half of the containment volume contains nearly all possible ignition sources and turbulence-promoting obstacles, the two points considered are believed to bracket all likely initiation points. The range of interest of oxygen concentration and initial temperature is shown in Fig. 1.

Axisymmetric pressures predicted for each postulated detonation at 15 evenly spaced points on the containment wall are presented in Ref. [4] as a function of dimensionless time, tC_o/r , where t = time since initiation, C_o = speed of sound in the un-burnt gas and r = internal radius of the cylinder and the dome. The non-dimensional pressure histories are valid for all containments geometrically similar to the one considered, i.e., with an internal height to radius ratio of 3.18. Peak wall pressures and computed specific impulses for all postulated detonations are listed in Table 1.

Examples of non-dimensional pressure histories presented in Fig. 2 display some typical features of the predicted wall pressure histories:

1. Initial shock reflection produces a pressure spike, usually followed by more spikes, sometimes higher than the first, which are caused by reflection of waves already reflected elsewhere,
2. For a detonation that starts at the floor (Fig. 2a and 2b) points of the cylinder experience their peak pressure and most of the impulse relatively late in the load history, after points at the dome have felt their peak pressures and most of their impulse. This can be explained by the fact that the original vertically propagating shock front and the waves obliquely reflected from the upper part of the cylinder converge and focus at the dome, causing a strong reflection around the apex (Fig. 2b). The reflected shock moves downwards, producing, in turn, large pressures at the bottom half of the cylinder (Fig. 2a).
3. A detonation starting at approximately containment mid-height produces a more spherical shock than the detonation with initiation at the floor. All points experience their peak pressures early in the load history and almost simultaneously. Because the stronger multi-directionality of the waves causes more scattering, dynamic pressures die out faster than for initiation at the floor.
4. Dynamic pressures decay to values of the order of 3 to 4 times the initial pressure, P_o , or less, within approximately 200msec for initiation at the bottom and in about 100msec for initiation at mid-height. (For the containment considered, the normalizing constant r/C_o in Fig. 2 equals 60msec). These final pressure values are close to the quasi-steady pressure rise expected after complete equilibration in the containment.

The predicted wall pressure histories are in qualitative agreement with those obtained in Ref. [1] by a Finite Difference approach, for slightly different geometry and dimensionless heat release rate. It is pointed out in Ref. 1 that because the numerical damping inherent in the Finite Difference procedure broadens the shock front, predicted peak pressures are smaller than theoretical values. This observation explains why the present method gives higher pressures in comparison to Ref. [1].

CONTAINMENT DYNAMIC RESPONSE

The axisymmetric dynamic analysis of the containment subjected to the computed pressure histories were performed in the time-domain by non-linear Finite Elements. Details of the analysis can be found in Refs [6] and [7].

Dynamic response analysis of the containment was performed for the following postulated detonations:

1. initiation at the floor with a detonation strength of $q/RT_o = 17$;
2. initiation at mid-height with $q/RT_o = 17$;
3. initiation at mid-height with $q/RT_o = 23$.

The initial internal pressure was taken equal to 1 atm (14.7 psia). The response was computed first assuming that the steel reinforcement has uniform properties equal to average values and that bar splices do not fail. In a second series of analysis reinforcement and splice variability was taken into account by using the effective stress-strain curves developed for ensembles of hoop or meridional and diagonal bars.

In the analysis which neglect material variability, both detonations with initiation at containment mid-height produce peak stresses of 595 Mpa in the hoop reinforcement at approximately one-third of containment height, about 85 msec after initiation (Fig 3). The maximum stresses are significantly smaller than the average high-strain-rate ultimate strength of the reinforcement. The location of maximum stresses is explained by the fact that the largest impulses caused by initiation at mid-height occur at the bottom half of the cylinder (Table 1). Initiation at the floor causes the reinforcement near the dome apex to reach the peak of its stress-strain law and rupture, approximately 90 msec after initiation (Fig. 3). Simultaneously occurring stresses in the hoop direction of the cylinder do not exceed yields (Fig. 3). This at first seems surprising, given that the impulses imparted on the bottom half of the cylinder within the first 85 msec are greater for initiation at the base than for initiation at mid-height (Table 1). The difference in the response can be explained by observing that for floor initiation early impulses and pressures are greater at the dome than at the bottom half of the cylinder (Fig. 2a and 2b). Therefore, initiation at the base excites, during the early part of the response in which dome failure occurs, those vibrational modes in which the dome participates most. (Ref. 6 shows that these can be the first two modes of the containment.) On the contrary, initiation at mid-height, which produces larger pressures and impulses at the bottom half of the cylinder than at the dome, excites mainly higher order modes (eg, the fourth and fifth, shown in Ref. 6), in which the cylinder participates most.

For accident conditions the initial containment pressure, P_o , will most likely exceed 1 atm. Given that the dynamic pressures due to detonation are proportional to P_o and that containment failure is predicted even for $P_o = 1$ atm, any of the three postulated detonations can be expected to cause failure for initial pressures higher than atmospheric.

EVALUATION OF APPROXIMATE PROCEDURES BASED ON PURE IMPULSE

In past analysis of the containment subjected to hydrogen detonation loading, the containment has been modelled as a single-degree-of-freedom (SDOF) system subjected to pure impulse loading [10,14]. For a SDOF system, a pure impulse analysis gives good results if the duration of loading is

at least one order of magnitude shorter than the natural period. For longer durations, the pure impulse assumption is conservative. In a pure impulse type of calculation, the maximum response of the system can be obtained by equating the strain energy stored in the system at the instance of peak response to the kinetic energy imparted to the mass m , of the system by the impulse. This kinetic energy can be computed by neglecting the resistance offered by the system during the short duration of loading converting the impulse I into an initial velocity I/m .

For initiation at containment mid-height, the response is maximum in the hoop direction between the bottom third and the middle of the cylinder. Therefore the appropriate SDOF model is an infinite cylinder vibrating in its axisymmetric mode and subjected to a uniform specific impulse, equal to the average specific impulse caused by the detonation over the bottom half of the cylinder (Table 1). For initiation at the base, response is maximum around the dome apex. Therefore the appropriate SDOF model is a spherical containment vibrating in its axisymmetric (breathing) mode, and subjected to a uniform specific impulse equal to the value computed at the apex (Table 1). For both SDOF systems, the kinetic energy imparted per unit surface of the wall by the specific impulse I equals $I^2 / \rho t_w$, where ρ = mass density and t_w = thickness of the wall. This kinetic energy is equated to the total strain energy in the liner and the reinforcement (hoop and meridional for the dome, hoop and seismic diagonal for the cylinder) per unit wall surface. Using the non-linear stress-strain relations of the liner and the reinforcement, this latter strain energy is expressed in terms of the peak dynamic strain of the SDOF system [6].

Using the procedure outlined above, the relationships between applied specific impulse and peak dynamic strain shown in Fig. 4 are obtained, for the containment analysed in this study. If the variability in steel properties and splice strengths is included, the approximate analysis predicts failure of the containment, which agrees with the finite element results. If the variability of reinforcement is neglected, the pure impulse predictions for the maximum strains are in very good agreement with the 1.82% value predicted by finite elements for initiation at mid-height. However, for initiation at the base the approximate procedure gives a peak strain at the apex of only 4.25%, whereas the finite element analysis predicts failure, i.e., exceedance of the 10% ultimate strain. This difference can be attributed to the fact that the SDOF model gives results which are averages in the meridional direction, being unable to capture any stress peaks associated with meridionally-varying stress fields. It is important to notice also that the good agreement of the approximate results for the cylinder with the Finite Element predictions is the result of compensating errors: The tendency of the SDOF procedure to underestimate the peak dynamic response of a multi-degree of freedom system on one hand, and the conservatism inherent in the pure impulse approximation for finite duration of loading, on the other.

In conclusion, an approximate procedure based on a pure impulse assumption and on idealisation of the containment as a SDOF system may be seriously unconservative and should be used with caution. In addition, selection of the appropriate SDOF model for use in such an analysis requires prior identification of the most critical region and the most likely failure mode. For these reasons, such an approximate procedure is not a good substitute for a detailed dynamic analysis.

The initial internal pressure was taken equals to 1 atm (14.7 psia). The response was computed first assuming that the steel reinforcement has uniform properties equal to average values and that bar splices do not fail. In a second series of analysis reinforcement and splice variability was taken into account by using the effective stress-strain curves developed for ensembles of hoop or meridional and diagonal bars.

CONCLUSIONS

If hydrogen detonation develops inside a nuclear reactor building, the pressure impulses generated by the detonation will result in the failure of the structure. The pressure histories were predicted by computing detonation as a sharp discontinuity using the random choice method. The response of the structure was performed in the time-domain by non-linear Finite Elements. An approximate

solution by simulating the containment by a single degree of freedom system (SDOF) is no conservative. This suggests that a detailed analysis is required for the reliable prediction of the containment response to loading from hydrogen detonation.

REFERENCES

1. Byers, R.K., CSQ Calculations of Hydrogen Detonations in Zion and Sequoyah, Workshop on the Impact of Hydrogen on Water Reactor Safety, Sandia National Laboratories, Albuquerque, N.M., Jan. 1981.
2. Chorin, A.J., Random Choice Methods with Application to Reacting Gas Glow, *Journal of Computational Physics*, Vol. 25, pp 253-272, 1977.
3. Cowell, W.L., Dynamic Tests of Concrete Reinforcing Steels, Technical Report R 394, U.S. Naval Civil Engineering Laboratory, Port Hueneme, CA, AD 622554, Sept. 1965.
4. Delichatsios, M.A. and Genadry, M.B., Calculations of Hydrogen Detonations in Nuclear Containment by the Random Choice Method, *Nuclear Engineering and Design*, Vol. 74, pp 117-126, 1982.
5. Fardis, M.N. and Buyukozturk, O., Shear Stiffness of Concrete by Finite Elements, *Journal of the structural Division, ASCE*, Vol. 106, No. ST6, Proc. Paper 14563, pp. 1311-1327, June 1980.
6. Fardis, M.N., Nacar, A., and Delichatsios, M.A., Reinforced Concrete Containment Safety under Hydrogen Detonations, Research Report R82-19, Department of Civil Engineering, Massachusetts Institute of Technology, Cambridge, MA, April 1982.
7. Fardis, M.N. and Nacar, A., Response of Reinforced Concrete Containments to Hydrogen Detonation, *Proceedings of the RLILEM-CEB-IABSE-IASS Symposium on Concrete Structures under Impact and Impulsive Loading*, W. Berlin, June 1982.
8. Glimm, J., Solutions in the Large for Nonlinear Hyperbolic Systems of Equations", *Communications in Pure and Applied Mathematics*, Vol. 18, pp 687, 1965.
9. Mainstone, R.J., Properties of Materials at High Rates of Straining or Loading, *Materiaux et Constructions*, Vol. 8, No. 44, March-April 1975, pp. 102-116.
10. Marks, J.C., Notes on Hydrogen Burn with Ignitors, Memorandum to ACRS members, U.S. Nuclear Regulatory Commission, Advisory Committee on Reactor Safeguards, Washington, D.C., Dec. 1980.
11. Mondkar, D.P., and Powell, G.H., ANSR-I: General Purpose programme for Analysis of Non-linear Structural Response, Report No. EERC, 75-37, Earthquake Engineering Research Center, University of California, Berkeley, CA, Dec. 1975
12. Shapiro, Z.M., and Moffettew, T.R., Hydrogen Flammability Data and Application to PWR Loss-of-coolant Accident, WAPD-SC-545, Bettis Plant, Sept. 1957.
13. U.S. Nuclear Regulatory Commission, Proceedings of Technology Exchange Meeting No. 5, and Zion Units 1 and 2, June 1980.
14. U.S. Nuclear Regulatory Commission, Reactor Safety Study, WASH-1400, Appendix VIII, Physical Processes in Reactor Meltdown Accidents, Dec. 1975.
15. Technology Review, MIT press ., May 2005
16. Shebeko Yu.N., Keller V.D., Yeremenko O.Ya., Smolin I.M., Serkin M.A., Korolchenko A.Ya., Regularities of formation and combustion of local hydrogen-air mixtures in a large volume, *Chemical Industry*, 1988, Vol.21, pp.24(728)-27(731) (in Russian).

Table 1. Peak detonation pressures and impulses on the containment wall

Location on wall		Initiation at the base $Q/RT_0=17$			$\frac{P_{max}}{P_0}$	Initiation at mid-height				
Radius (m)	Elevation (m)	$\frac{P_{max}}{P_0}$	Impulse (sec) $\frac{P_o}{P_0}$			a/RT=17		Q/RT ₀ =23		
			At 85 msec*	At 140 msec*		Impulse (sec) $\frac{P_o}{P_0}$		$\frac{P_{max}}{P_0}$	Impulse (sec) $\frac{P_o}{P_0}$	
					At 85 msec*	At 140 msec*	At 85 msec*		At 140 msec*	
20.6	0.0	77.0	0.56	1.18	72.0	0.75	0.81	76.0	0.63	0.63
20.6	6.0	72.0	0.82	1.35	75.0	0.70	0.78	78.0	0.51	0.51
20.6	12.0	51.0	0.74	1.24	51.0	0.67	0.73	80.0	0.59	0.59
20.6	18.0	48.0	0.72	0.97	55.0	0.61	0.68	46.0	0.40	0.40
20.6	94.0	37.0	0.65	0.85	70.0	0.37	0.46	66.0	0.51	0.51
20.6	30.0	30.0	0.62	0.88	58.0	0.39	0.45	68.0	0.50	0.50
20.6	36.0	48.0	0.63	0.81	49.0	0.35	0.40	48.0	0.41	0.41
20.6	42.0	42.0	0.52	0.73	21.0	0.25	0.25	26.0	0.38	0.38
20.5	47.0	43.0	0.37	0.56	34.0	0.25	0.25	41.0	0.35	0.38
14.7	51.0	42.0	0.90	1.24	27.0	0.22	0.22	30.0	0.31	0.33
17.5	56.0	71.0	0.58	0.75	41.0	0.19	0.19	48.0	0.19	0.19
13.1	61.0	65.0	0.64	0.79	25.0	0.26	0.26	34.0	0.21	0.22
9.3	63.5	71.0	0.49	0.63	59.0	0.40	0.41	71.0	0.33	0.33
5.3	65.0	68.0	0.50	0.66	23.0	0.42	0.44	32.0	0.31	0.31
0	65.7	65.0	0.76	1.11	69.0	0.46	0.55	53.0	0.44	0.46

Note * Time measured from the point of detonation initiation

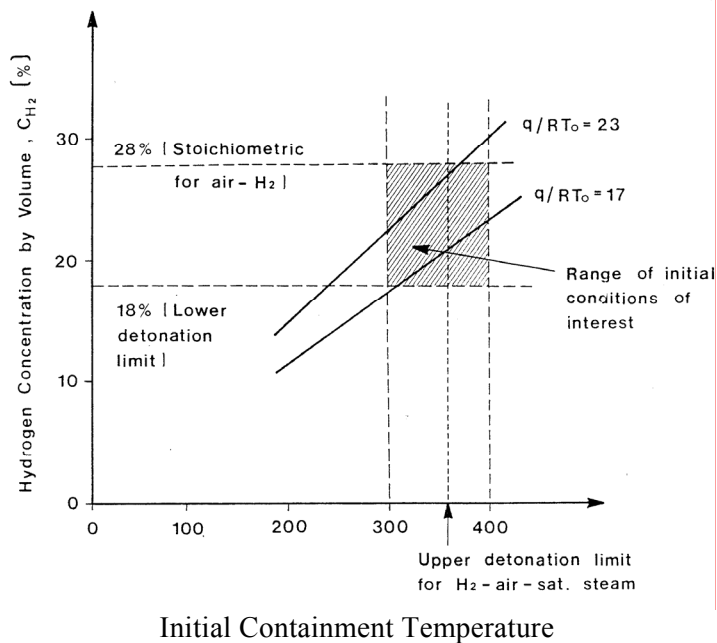


Figure 1. Range of interest of hydrogen concentration and initial temperature inside containment.

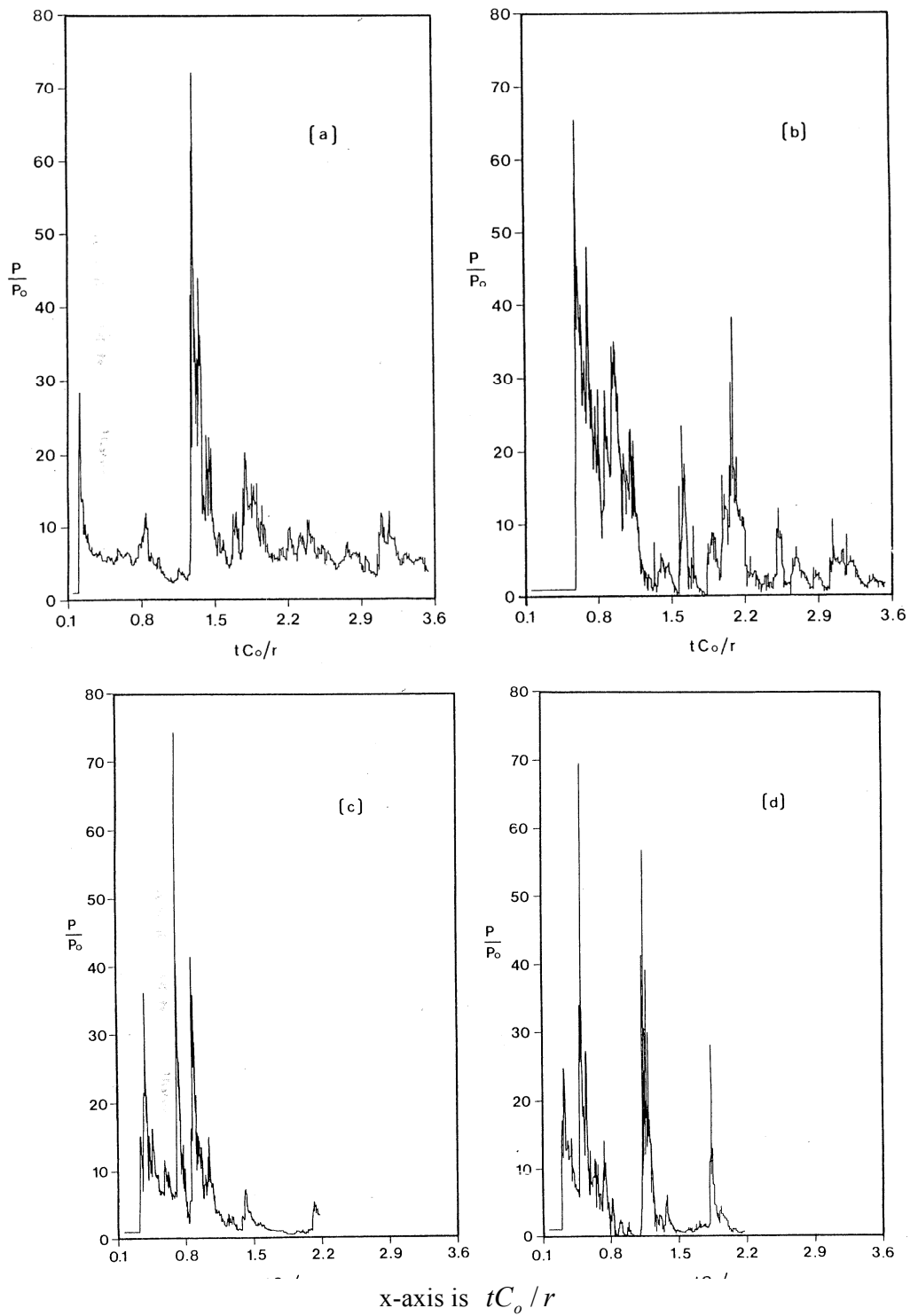


Figure 2 Representative wall pressure histories due to detonation with $\frac{q}{RT_0}=17$: (a) at 6m abovebase, for initiation at floor centre; (b) at dome apex, for initiation at floor centre; (c) at 6m above base, for initiation at midheight; (d) at dome apex, for initiation at midheight

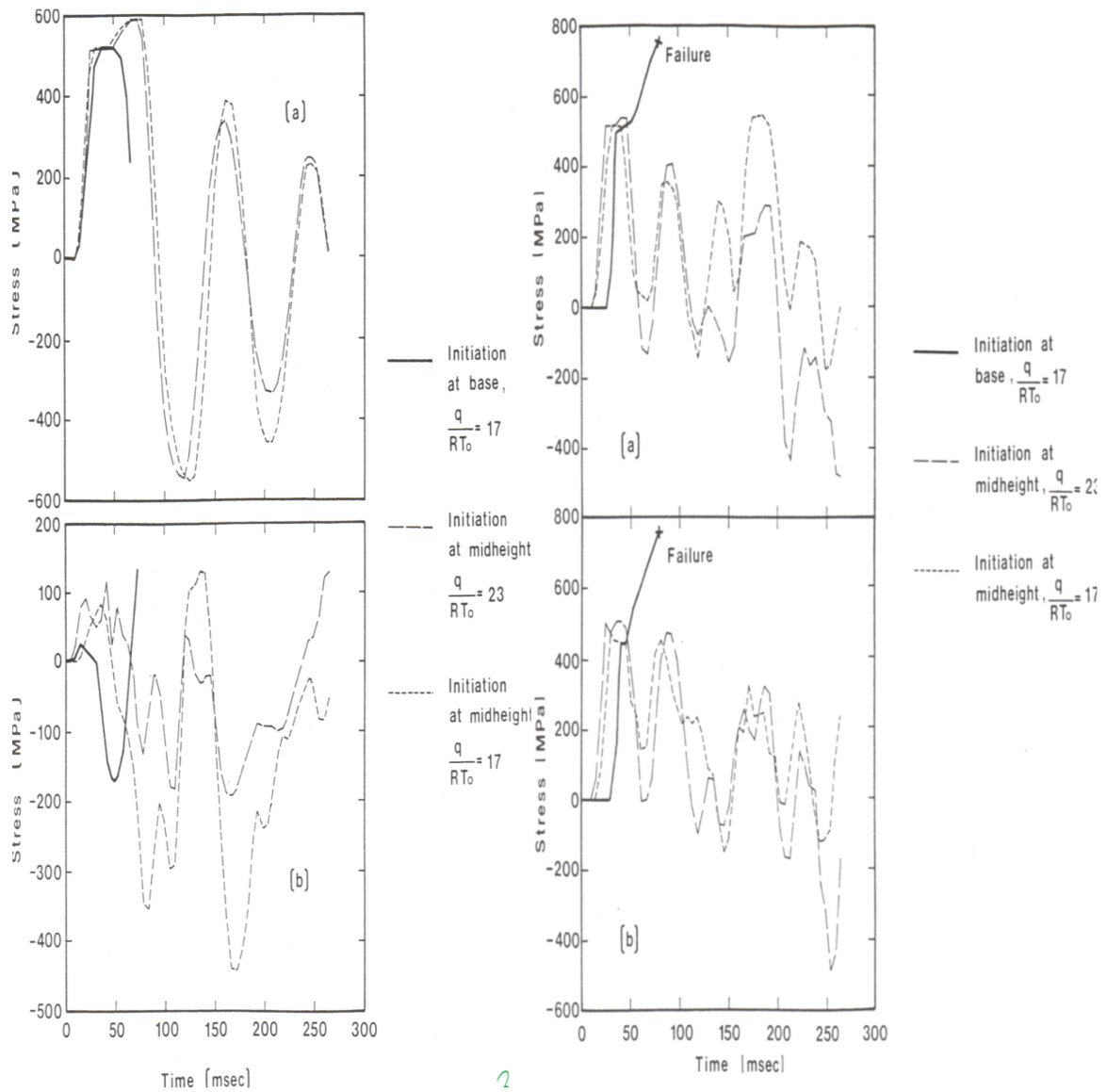


Figure 3 Left: Stress histories at 40% of cylinder height, with variation of steel properties neglected: (a) inside hoop bars; (b) inside vertical bars.

Figure 3 Right: Stress histories 10° from dome apex, with variation of steel properties neglected: (a) inside hoop bars; (b) inside meridian bars.

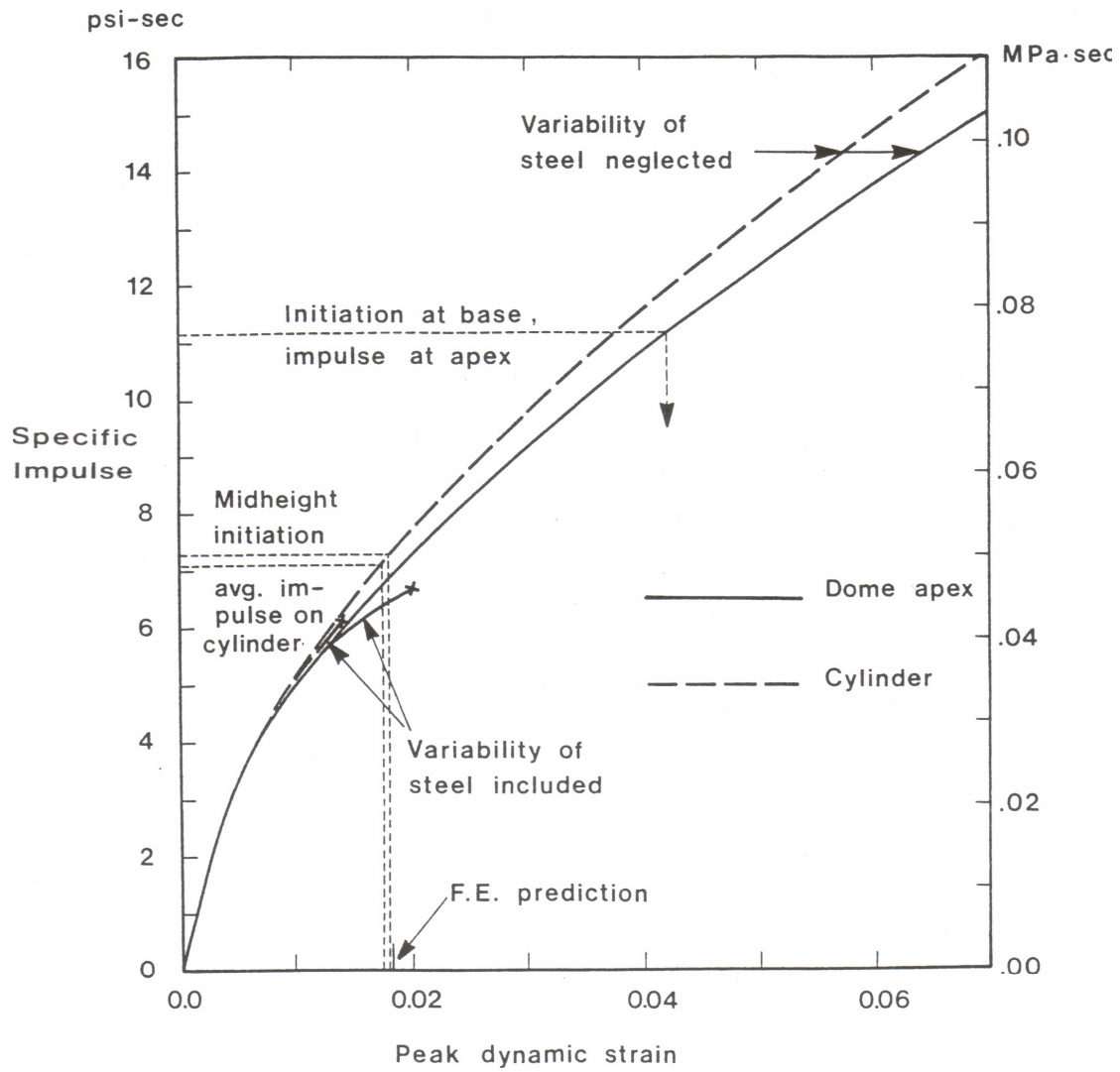


Figure 4. Approximate impulse-peak dynamic response relationship.